Modulation of Protonation−Deprotonation Processes of 2-(4′-Pyridyl)benzimidazole in Its Inclusion Complexes with Cyclodextrins

ARTICLE *in* THE JOURNAL OF PHYSICAL CHEMISTRY B · JUNE 2013

Impact Factor: 3.3 · DOI: 10.1021/jp403476n · Source: PubMed

THE JOURNAL OF PHYSICAL CHEMISTRY B

Article

pubs.acs.org/JPCB

Modulation of Protonation–Deprotonation Processes of 2-(4′-Pyridyl)benzimidazole in Its Inclusion Complexes with Cyclodextrins

Vijaykant Khorwal,[†] Biswajit Sadhu,[‡] Arghya Dey,[†] Mahesh Sundararajan,*[,§] and Anindya Datta*[,†]

[†]Department of Chemistry, Indian Institute of Technology Bombay, Powai, Mumbai 400 076, India

[‡]Radiation Safety Systems Division and [§]Theoretical Chemistry Section, Bhabha Atomic Research Centre, Mumbai 400 085, India

Supporting Information

ABSTRACT: 2-(4′-Pyridyl)benzimidazole (4PBI) can exist in several states of protonation, having three basic nitrogen atoms. The equilibria involving these states, in ground as well as in excited states, are found to be affected significantly by cyclodextrins (CDs). The formation of inclusion complexes of this compound with all three varieties of cyclodextrins is observed to be more favorable at pH 9 than at pH 4, due to the predominance of the neutral form of dye at pH 9. The binding affinity of 4PBI to CDs is found to be governed by two factors: (i) the size of the host and (ii) the mode of insertion of 4PBI. We find that, for the host with a smaller cavity (α-CD), insertion of the dye with a pyridyl face is favored, whereas, for γ-CD, the preference is shifted toward the benzimidazole face of the dye. For β-CD, the binding affinity of the dye is maximum due to perfect cavity matching with the guest. A combination of steric factor and hydrogen bonding interaction is found to be responsible for modulation of the protonation–deprotonation equilibria of the guest molecule in the inclusion complex. Surprisingly, a protonated form is found to be promoted upon inclusion in cyclodextrins, under certain conditions. This is an unusual behavior and has been rationalized by prototropism involving the hydroxyl protons of cyclodextrin molecules.

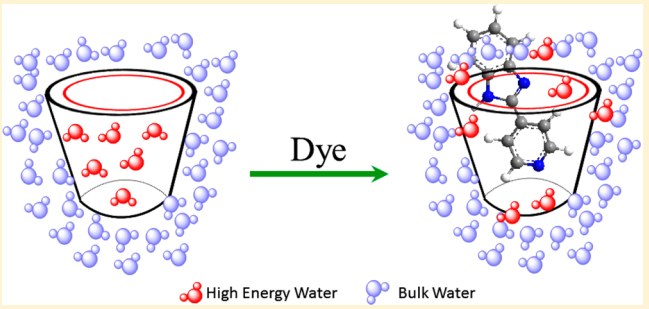

1. INTRODUCTION

Benzimidazole derivatives can undergo excited state proton transfer (ESPT) and exhibit interesting photophysical and photochemical properties.[1−5] The processes are extremely fast and have potential applications in the fields of lasers, photostabilization of polymers, and development of fluorescence sensors.[6−10] 2-(4′-Pyridyl)benzimidazole (4PBI) is a molecule of this family, which exhibits dual fluorescence. The photophysics of this molecule has been studied in aqueous and non-aqueous solutions by Rodriguez-Prieto and co-workers.[11−13] Depending on the pH of the medium, several species with varied degrees of protonation have been observed for this molecule. These are the neutral molecule **N**; monocation **C**, protonated at the second benzimidazole nitrogen atom; tautomer **T**, protonated at the pyridyl nitrogen atom instead of the second benzimidazole nitrogen atom; dication **D**, protonated at both nitrogen centers; and anion **A**, in which no nitrogen atom is bonded with a hydrogen atom (Scheme 1). The pK_a values of **C** and **T** (denoted as pK_{CN} and pK_{TN}, respectively) are 4.2, implying that the basicities of both pyridyl and benzimidazole nitrogens are the same in the ground state. The excited state pK_a values (pK_{CN}* and pK_{TN}*, respectively), however, are 4.8 and 14, respectively, implying that the basicity of the benzimidazole nitrogen atom does not change significantly upon excitation but that of the pyridyl nitrogen is significantly more basic in the electronically excited state of the molecule.[12]

Even though the photophysics of 4PBI in aqueous and non-aqueous solutions has been studied in detail, there has been no study in restricted microenvironments so far, except from our very recent studies of 4PBI in micelles.[14] Such studies promise to be interesting, as has been manifested in earlier reports on the excited state proton transfer of another benzimidazole derivative, 2-(2′-pyridyl)benzimidazole (2PBI).[15−18] This is the motivation behind the present study on the fluorescence properties of 4PBI in cyclodextrins (CD), which are cyclic oligosaccharides consisting of six, seven, and eight glucose units for α-, β-, and γ-CD, respectively, linked by α-1,4-glycosidic bonds. The internal diameters of these CDs are 4.9, 6.2, and 7.9 Å, respectively.[19] The disposition of the −OH groups in the glucose units is such that the outer surface of a CD molecule is polar and the inner surface is apolar. By virtue of this structure, CDs exhibit a remarkable ability to form inclusion complexes with a variety of organic compounds in aqueous solutions.[20−23] The formation of such inclusion complexes results in the rearrangement of molecule and removal of water from CD cavity.[24] The major driving force for the inclusion phenomenon is van der Waals and hydrophobic interaction between the CD framework and a guest molecule. Besides, dipole−dipole interaction, charge transfer and electrostatic interactions,

Received: April 9, 2013
Revised: May 29, 2013
Published: June 3, 2013

dx.doi.org/10.1021/jp403476n | J. Phys. Chem. B 2013, 117, 8603−8610

Scheme 1. Different Forms of 4PBI and a Schematic Representation of Cyclodextrins (CDs) and 4PBI

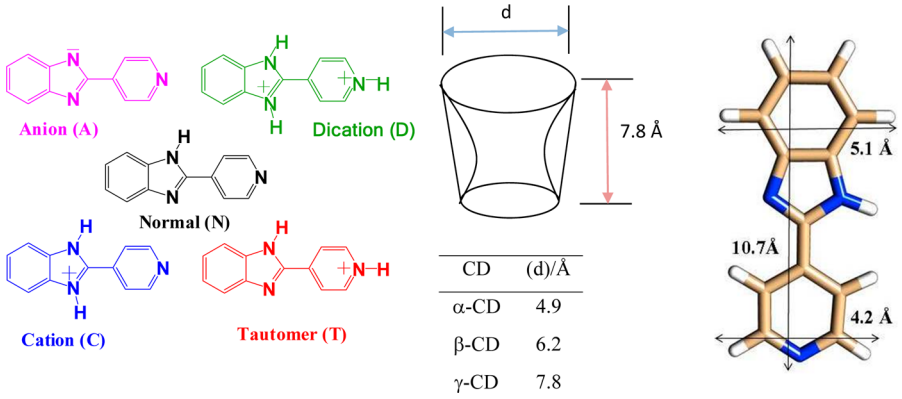

CD	(d)/Å
α-CD	4.9
β-CD	6.2
γ-CD	7.8

along with hydrogen bonding and steric effects also play crucial roles here.[25] The incorporation is often in a manner such that the less polar part of the guest molecule is included in the cavity while the more polar or charged moiety faces or even protrudes out.[26] This phenomenon has potential applications in catalysis, photochemistry, drug delivery, analytical chemistry, and as models for molecular recognition phenomena like enzyme−substrate or drug target interaction.[27] CDs can be used as a toxicity reducing agent and in pesticide formulations, by forming complexes with water insoluble or less soluble molecules, that biodegrade readily in their uncomplexed forms.[28] For fluorescent guests, a marked augmentation in fluorescence intensity is generally observed upon inclusion in CDs.[29−41] This may be ascribed to shielding from water molecules as well as incorporation in an apolar, rigid microenvironment.

It is surprising, in this context, that there is only one study of the interaction of the molecule of the PBI family with CDs.[15] In this study, the host−guest complex formation of 2PBI has been found to be favored in the case of α-CD rather than in the case of β-CD and γ-CD, presumably because of the mismatch of the size of 2PBI with the larger cavity of β-CD and γ-CD.[15] Binding with α-CD hinders the ESPT process in 2PBI at pH 4. With this background, we present our studies on 4PBI in CDs at pH 4 and 9. Particularly, we want to examine if the extent of shift in the protonation−deprotonation equilibria is observed due to inclusion in macrocyclic hosts by using a combined experimental and quantum chemical calculations. We believe that combining experimental and computational methods can give additional insights into the structure−function relationship of host−guest complexes. Such synergetic studies are particularly quite popular in other branches of chemistry; however, in supramolecular host−guest complexes, quantum chemical calculations are scarce due to the large size of the system to be handled at high accurate quantum chemical level and the requirement of treating dispersion effects which are central to host−guest interactions. Fortunately, the empirical dispersion correction to the existing density functional theory (DFT) methods is now recognized to be an ideal choice for supramolecular host−guest interactions. In this regard, we have used the dispersion corrected DFT methods to understand the binding affinities of 4PBI with CDs.

2. EXPERIMENTS AND METHODS

2-(4′-Pyridyl)benzimidazole (4PBI) has been purchased from Alfa Aesar and purified by repeated recrystallization from ethanol/water mixture.[43] CDs from Aldrich have been used as received. Double distilled water is used to prepare the solutions. $HClO_4$ and NaOH are used to adjust the pH of the solution, and pH has been measured on a pH meter of model S2K712 from ISFETCOM, Japan. The absorption and fluorescence spectra have been recorded on a JASCO V530 and Varian Cary Eclipse spectrophotometer/spectrofluorimeter, respectively. Fluorescence decays have been recorded on a time correlated single photon counting (TCSPC) system from IBH with excitation by a pulsed light emitting diode (NanoLED, λ_{ex} = 295 nm). The full width at half-maximum of the instrument function is 700 ps. The emission polarizer has been kept at a magic angle polarization of 54.7° with respect to the polarization of the excitation light. The decays have been fitted to multiexponential functions by an iterative reconvolution method using IBH DAS v6.0 software.[44] The fitting functions are of the form

$$I(t) = I(0) \sum_i a_i \exp(-t_i/\tau)$$

where $I(t)$ and $I(0)$ are intensities at time t and 0, after excitation pulse of light. a_i and τ_i are the amplitude and lifetime of the ith component. All experiments are carried out at 25 °C.

The complexation of 4PBI to three CDs is explored through dispersion corrected DFT based calculations. Geometry optimizations of all species are carried out using the BP86-D (D2 correction) functional with the def2-SV(P) basis set for all atoms, while single point energy calculations on the optimized structures have been performed at the B3LYP-D/TZVP level using TURBOMOLE V6.0 2009.[45] The energies are further corrected for solvent effects by using the dielectric constant of water using the COSMO continuum solvation model. The above-mentioned strategy was successfully applied to understand the photophysical properties of CD−oxazine host−guest systems.[41]

The equation is used to determine the stoichiometry of the complex is[35]

$$\phi_f = \frac{(\phi_0 + \phi_1 K_1[\mathrm{CD}] + \phi_2 K_2[\mathrm{CD}]^2)}{(1 + K_1[\mathrm{CD}] + K_2[\mathrm{CD}]^2)}$$

where ϕ_0, ϕ_1, and ϕ_2 are the fluorescence quantum yields of the free fluorophore, 1:1 complex, and 1:2 complex, respectively. The values of ϕ_0 and k_1 from Benesi−Hildebrand analysis are used as constants in the equation. The binding constants and the quantum yields are then calculated by iterative nonlinear least-squares regression.

dx.doi.org/10.1021/jp403476n | J. Phys. Chem. B 2013, 117, 8603−8610

3. RESULTS

The absorption spectrum of 4PBI consists of a single band at 310 nm at pH 9, due to the **N** form. At pH 4, an additional band is observed at 350 nm, due to the formation of **T**. The 310 nm band at pH 4 is ascribed to **C** rather than **N**.[12] The absorption spectra at pH 4 as well as pH 9 do not change upon addition of α-CD (Figure 1). However, the **T** absorption at 350

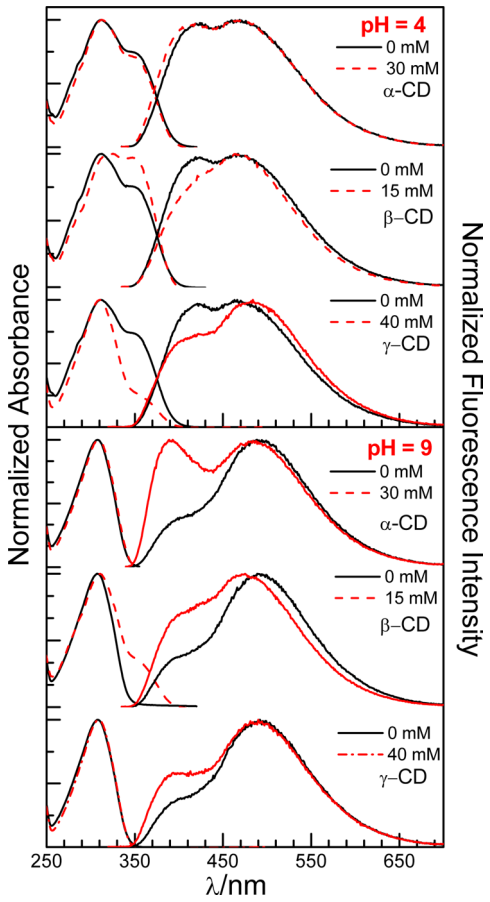

Figure 1. Normalized absorption and emission spectra of an aqueous solution of 4PBI in the absence (solid line) and presence (dashed line) of α-CD, β-CD, and γ-CD at pH = 4 (upper) and pH = 9 (d, e, and f) (lower).

nm becomes more prominent upon addition of β-CD, at both values of pH. In contrast, the **T** band becomes weaker in the presence of γ-CD at pH 4, while the spectrum remains unchanged at pH 9. The fluorescence spectra at pH 4 as well as 9 exhibit two bands at 380 nm (**N*** and **C*** emission) and 490 nm (**T*** emission). The contribution from the two bands is the same at pH 4, but **T***emission is significantly stronger than **N*** emission at pH 9. Upon addition of α-CD, the fluorescence spectra remain unaltered at pH 4. At pH 9, however, there is a significant increase in the **N*** emission, while the intensity of **T*** emission undergoes a very small decrease (Figures 1 and 3A and Figure S2, Supporting Information). Upon addition of β-CD at pH 4, **T*** emission undergoes a small but perceptible increase. At pH 9, on the other hand, the total fluorescence intensity increases (Figure S4, Supporting Information), with an increase in the contribution from **N*** emission and a slight blue shift of both the **N*** and **T*** bands (Figures 1 and 3B and Figure S4, Supporting Information). In the case of γ-CD, there is a decrease in the total fluorescence intensity at pH 4 (Figure S6, Supporting Information). Moreover, the decrease in the **C*** emission takes place to a relatively greater extent (Figures 1 and 3C). At pH 9, on the other hand, **N*** emission becomes stronger at the expense of **T*** emission at pH 9 (Figures 1 and 3C and Figure S6, Supporting Information).

Fluorescence decays have been recorded at two different emission wavelengths, 380 and 490 nm, corresponding to **N***/**C*** and **T*** emission, respectively. At pH 4, all decays are biexponential at λ_{em} = 380 nm, with lifetimes of 0.20 and 5.80 ns and amplitudes of 0.78 and 0.22, respectively. The shorter lifetime is assigned to **N*** and the longer to **C***. Henceforth, in the present article, amplitudes have been denoted within parentheses, after the respective lifetime. Upon addition of CDs, the shorter lifetime increases to 0.73 ns (0.80), 0.60 ns (0.77), and 0.54 ns (0.91), in the case of α-, β-, and γ-CD, respectively. The longer lifetime has values of 5.45, 5.60, and 4.58 ns, respectively (Table 1). At pH 9, the major component

Table 1. Temporal Characteristics of 4PBI in Its Inclusion Complex with Cyclodextrins in Aqueous Solution at pH 4 and 9

pH	CD	concentration (mM)	λ_{em} (nm)	species	τ (ns)	amplitude
4	aqueous solution of 4PBI		380	N*	0.20	0.78
				C*	5.80	0.22
			490	T*	5.0	
	α	35	380	(N-α-CD)*	0.73	0.80
				C*	5.45	0.20
			490	T*	4.82	
	β	15	380	(N-β-CD)*	0.60	0.77
				C*	5.60	0.23
			490	T*	4.94	
	γ	40	380	(N-γ-CD)*	0.54	0.91
				C*	4.58	0.09
			490	T*	4.65	
9	aqueous solution of 4PBI		380	N*	0.15	0.99
				A*	1.39	0.01
			490	T*	4.26	
	α	35	380	(N-α-CD)*	0.30	0.95
				A*	1.31	0.05
			490	T*	4.30	
	β	15	380	(N-β-CD)*	0.41	0.94
				A*	5.40	0.06
				T*	4.70	
	γ	40	380	(N-γ-CD)*	0.25	0.93
				A*	1.45	0.07
			490	T*	4.45	

at λ_{em} = 380 nm is of 0.15 ns (0.99). A component of 1.39 ns is also observed, with very low amplitude. Upon addition of α-CD, the shorter lifetime increases to 0.30 ns (0.95). The corresponding values of lifetime in the case of β- and γ-CD are 0.41 and 0.25 ns, respectively, with decreasing contribution to 0.94 and 0.93, respectively. The longer lifetime is almost constant in α- and γ-CD but increases to 5.40 ns in β-CD. The decays at 490 nm emission at both values of pH are single exponential with a lifetime of 5.0 ns pH 4 and 4.26 ns at pH 9.The lifetime at pH 4 decreases slightly upon addition of CDs. For solutions with pH 9, however, it increases slightly upon incorporation in CDs (Figure 2, Figure S7, Supporting Information, and Table 1).

dx.doi.org/10.1021/jp403476n | J. Phys. Chem. B 2013, 117, 8603−8610

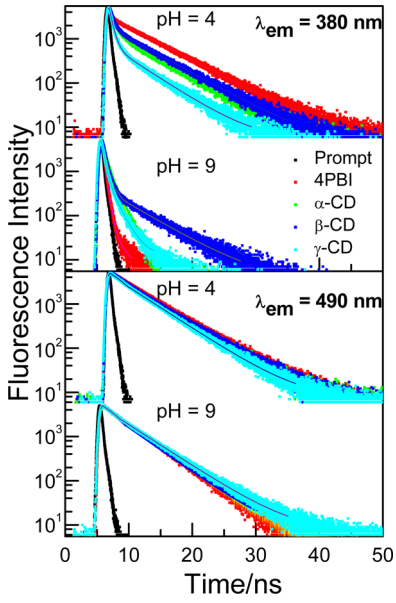

Figure 2. Fluorescence decay in an aqueous solution of 4PBI at pH = 4 and 9, at the highest concentration of cyclodextrins with λ_{em} = 380 and 490 nm and λ_{ex} = 295 nm.

The encapsulation of 4PBI to the CD cavity has been examined computationally. Prior to the host−guest complexation results, it is informative to explore the properties of the different forms of 4PBI. In the present study, all three forms are found to be planar (Scheme 1). The **T** form is energetically more favorable as compared to the **C** form in the ground state by only 2 kcal mol^{-1}. While exploring the binding of 4PBI to the three CDs, the pyridyl (P) and benzimidazole (BI) binding mode of all three forms (**N**, **C**, and **T**) to three CD host molecules have been considered. The diameters of pyridyl and benzimidazole heterocyclic rings of 4PBI suggest that both of the binding modes are feasible, particularly for β- and γ-CDs. Due to steric reasons, only the pyridyl part of 4PBI can interact with α-CD. The binding energies and proton affinities are calculated using the following two equations:

$$\text{CD} + \text{4PBI} \rightarrow \text{4PBI–CD}$$

$$\text{4PBI} + \text{H}_3\text{O}^+ \rightarrow \text{4PBI–H}^+ + \text{H}_2\text{O}$$

The calculated binding energy and proton affinities are listed in Tables 3 and 4. The optimized structures of host−guest complexes have been shown in Figure 5.

4. DISCUSSION

The ground state of 4PBI consists of a mixture of **N** and **C** at pH 9. At pH 4, **T** is also present along with **N** and **C**, as is evident in the absorption spectra (Figure 1). This observation is in keeping with the pK_a values reported in the literature.[12] The calculated ground state relative energies of **T** and **C** of bare 4PBI are very close with the marginal preference to the **T** form (~2 kcal mol^{-1}) consistent with the experimental observation. Interestingly, different CDs have different effects on the relative populations of these forms. α-CD has no effect on the absorption spectra (Figure 1 and Figure S1, Supporting Information), implying that it is unable to affect the ground state protonation−deprotonation equilibria to any significant extent. However, this does not necessarily imply that 4PBI does not bind to α-CD. Quantum chemical calculations indicate that all three forms of 4PBI bind with α-CD (Figure 5, Table 3). The binding of 4PBI with α-CD through the pyridyl part is expected to be more favorable as compared to the benzimidazole part due to the smaller cavity size of the host. The calculated binding energy of 4PBI in α-CD is larger for all three forms (**N**, **C**, and **T**) for binding through the pyridyl part. The binding of the **N** form is more favorable as compared to cationic **C** and **T** forms (Table 3). An experimental manifestation of the binding is obtained in the increase in 380 nm fluorescence upon incorporation in α-CD, with a concomitant slight decrease in the 490 nm (**T***) fluorescence. Thus, it appears that **N*** to **T*** ESPT is hindered upon confinement in α-CD. The changes in the fluorescence spectrum at pH 4 are negligible, confirming the nonoccurrence of ESPT at this pH. This is rationalized by the fact that, at this pH value, **C** rather than **N** is present and **C*** to **T*** ESPT does not occur in 4PBI.[14]

β-CD is found to promote the formation of **T** in the ground state, in preference over **N**, at both pH values (Figure 1). The preference for a protonated form is surprising *prima facie*, as one would generally expect the neutral form to bind to CDs more efficiently than the cationic form, considering hydrophobic interactions alone.[26] However, from the computational results, we find that both the **C** and **T** forms bind more strongly as compared to the **N** form. Further, the binding affinities are equally strong for both the pyridyl part and the benzimidazole part to β-CD for the **C** form. The stronger binding of 4PBI in the **C** form is largely due to the strong hydrogen bonding between the protons attached to the nitrogen of the benzimidazole ring with the hydroxyl groups present in CD. The **T** form could be easily formed, as the nitrogen of the pyridyl ring can abstract the protons from the solvent water molecules.

The **C** form is found in a greater extent upon incorporation in γ-CD. However, **T*** fluorescence is significant in this system, implying the occurrence of ESPT within this macrocyclic cavity. Quantum chemical calculations reveal that, in γ-CD, the binding of 4PBI is stronger with the **C** form with both the benzimidazole part and the pyridyl part. Within the two binding modes, the benzimidazole part binds stronger (5 kcal mol^{-1}) as compared to the pyridyl part (Table 3). The cavity size of γ-CD is very large, so the binding is dominated by hydrophobic interaction which is very loose for 4PBI. However, for α-CD, the interaction is only through hydrogen bonding, whereas, in β-CD, the binding of 4PBI is dominated by both hydrophobic interactions and hydrogen bonding.

The relative quantum yield of **N** with respect to **T** (pH 9) increases upon increasing the CD concentration, for α-, β-, as well as γ-CD (Figure 3). The relative quantum yield of **C** with respect to **T** (pH 4), however, depends on the nature of the CD. The ratio is almost constant in α-CD but decreases upon incorporation of 4PBI in β-CD and γ-CD. The overall fluorescence intensity decreases upon increasing the concen-

Table 2. Steady State Fluorescence Parameters of 4PBI in Its Inclusion Complexes with the Supramolecular Hosts and the Binding Constants, Obtained from Figure 4

	binding constant (pH 9)		binding constant (pH 4)	
system	K_1 (mM^{-1})	K_2 (mM^{-1})	K_1 (mM^{-1})	K_2 (mM^{-1})
α-CD	51.98	5.27	1.65	0.08
β-CD	70.70			
γ-CD	10.02	3.54		

dx.doi.org/10.1021/jp403476n | J. Phys. Chem. B 2013, 117, 8603−8610

Table 3. Calculated Binding Affinities (kcal mol^{-1}) of 4PBI to CDs

	α-CD		β-CD		γ-CD	
	pyridyl	benzimidazole	pyridyl	benzimidazole	pyridyl	benzimidazole
neutral	−15.1	−5.0	−10.7	−5.9	−8.8	−3.4
cation	−14.7	−11.9	−15.0	−14.7	−9.6	−13.4
tautomer	−12.8	−12.4	−6.0	−13.9	−4.1	−6.5

Table 4. Calculated Proton Affinities (kcal mol^{-1}) of 4PBI[a]

	C/P	C/BI	T/P	T/BI
α-CD	−24.6	−30.0	−25.0	−29.7
β-CD	−29.3	−31.9	−26.2	−31.9
γ-CD	−22.2	−30.5	−22.6	−25.5

[a]C/P, cation/pyridyl part; C/BI, cation/benzimidazole part; T/P, tautomer/pyridyl part; T/BI, tautomer/benzimidazole part.

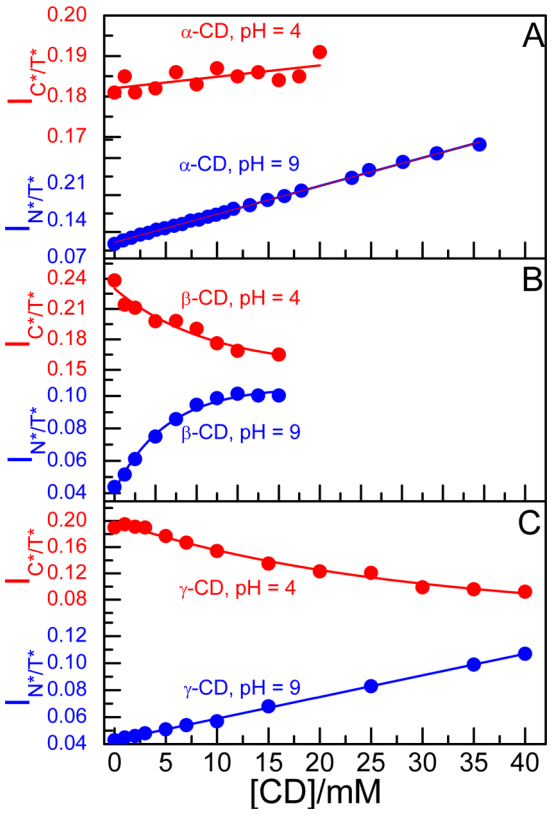

Figure 3. Relative quantum yield (ϕ_f) of 4PBI against the [CD] in water with varying concentrations of (A) α-CD at pH 4 (red circles) and pH 9 (blue circles), (B) β-CD at pH 4 (red circles) and pH 9 (blue circles), and (C) γ-CD at pH 4 (red circles) and pH 9 (blue circles). The points represent experimental values, and the solid lines represent the nonlinear least-squares fit.

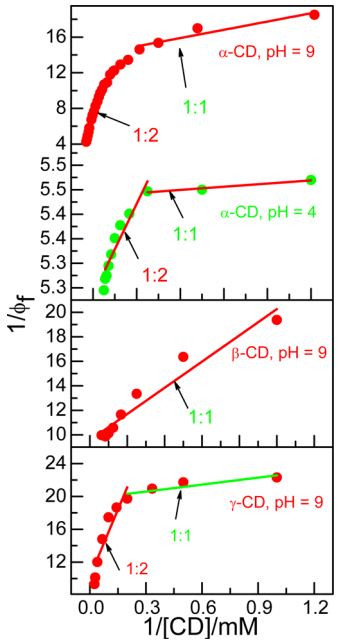

Figure 4. Benesi−Hildebrand plots for determination of the binding constants of 4PBI with the supramolecular hosts. The two linear plots in the different concentration ranges in cases α-CD, β-CD, and γ-CD denote two kinds of stoichiometry: 1:1 at low concentrations and 1:2 at higher concentrations of cyclodextrins.

tration of γ-CD in aqueous solution of 4PBI at pH 4 (Figure S6, Supporting Information). This may be rationalized in the light of a greater ground state population of the **N** form in complexes with γ-CD. The relative increase in the **T*** emission may be explained as a result of ESPT from **N*** to **T***. The dye is deeply embedded inside the β-CD and γ-CD cavities due to the larger size of these macrocycles. In the case of β-CD, the interaction of the pyridyl part of the dye with the secondary −OH group of the CD cavity, at pH 4, causes the intensity of the 380 nm (**C***) peak to decrease, perhaps due to formation of an exclusion complex, as observed earlier with oxazine-1.[41] The 490 nm (**T***) emission is augmented (Figure S4, Supporting Information), seemingly due to the exposure of the pyridyl part of the dye from the other side of the CD cavity and ESPT *via* water molecules. In the case of γ-CD, the intensity of emission of the **C*** and **T*** forms decreases at pH 4, due to loss of binding of the guest molecule. At pH 9, the intensity of the **T*** band decreases and the band present at 380 nm (**N***) gains intensity upon addition of γ-CD (Figure S6, Supporting Information). This is due to the formation of an inclusion complex with the **N** form of the dye.

Along with binding affinity calculation, we have also calculated the proton affinity (Table 4) of the **C** and **T** forms of 4PBI and its complexes with CD. The computed ground state proton affinities of 4PBI bound species depend on three factors: (i) mode of insertion of 4PBI, (ii) cavities of host, and (iii) relative stabilization of three forms of guests. For α-CD, the proton affinities of 4PBI of the **C** and **T** forms are identical, whereas, for β-CD, the **C** form is favored with the pyridyl part. For the larger γ-CD, the proton affinity of the C form is favored by 5 kcal mol^{-1} with the benzimidazole part. We have estimated the excited state proton affinity (ESPT) using time-dependent DFT with the B3LYP functional with TZVP basis in the gas phase. Due to the apparent large size of the system (>150 atoms), we were unable to carry it out with solvent effects. Nevertheless, we note that, irrespective of the cavity size of the host, the **T** form is largely favored as compared to the **C** form

dx.doi.org/10.1021/jp403476n | J. Phys. Chem. B 2013, 117, 8603−8610

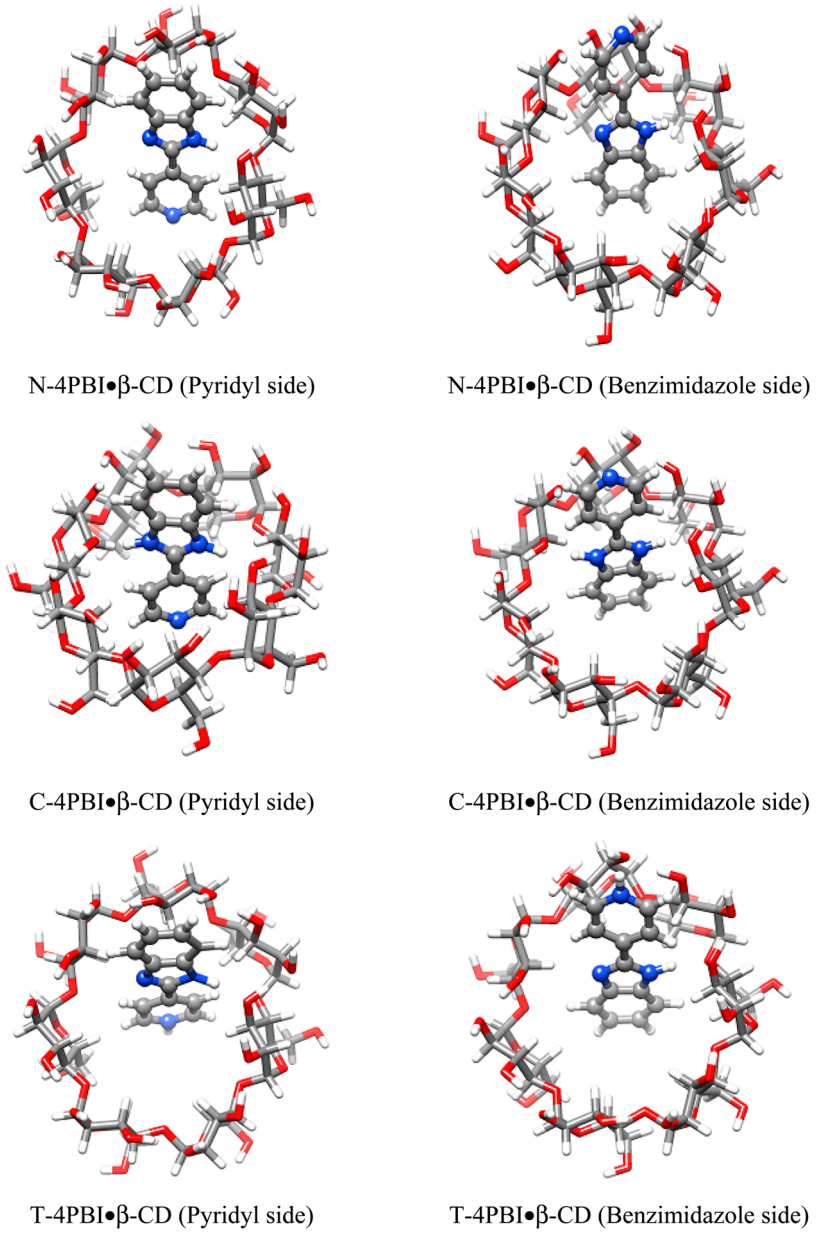

Figure 5. Geometry-optimized structures of host−guest complexes of 4PBI and β-CD.

consistent with our experimental data (Table S1, Supporting Information).

According to the Benesi−Hildebrand equation, a plot of $1/\phi_f$ against 1/[CD] exhibits an upward curvature in the case of α-CD at both pH's and in the case of β-CD and γ-CD at pH 9. A downward curvature is observed in the case of β-CD and γ-CD at pH 4. In α-CD at both pH values, the complex stoichiometry is 1:1 at low CD concentrations. Upon increasing the concentration of α-CD, the stoichiometry of the complex is 1:2, which is the same as that with γ-CD at pH 9. In β-CD, the stoichiometry is 1:1 at all concentrations of CD used (Figure 4, Table 2).

The lifetime of the **N*** increases due to complex formation with cyclodextrins (Table 1). The lifetime at 490 nm emission decreases upon complexation, possibly because of a more efficient deactivation of the excited state of the cationic species in the hydrophobic environment. At pH 9, the lifetime of **N*** increases to 0.30, 0.41, and 0.25 ns in α-CD, β-CD, and γ-CD, respectively, with constant amplitude. This clearly indicates the formation of inclusion complexes between **N*** and the host molecules. The lifetime of the **T*** form at this pH does not change appreciably in α-CD, but in the case of β-CD and γ-CD, it increases to 4.70 and 4.45 ns, respectively. This is due to the loose binding of the dye with the host, leading to a significantly less dynamic quenching of **T*** in these inclusion complexes. At pH 9, the lifetime at 380 nm emission in the case of β-CD increases to 5.40 ns, which is due to the **C*** form of the dye. This issue can be rationalized by the consideration of the quantum chemical calculation which reveals that the binding of the **C** form of the dye to β-CD is more as compared with **N** and **T** and thus **C*** is more abundant in inclusion complexes with β-CD (Figure 2, Figure S7, Supporting Information, and Table 1). The favorable host−guest complexes can be explained on the basis of the extent of charge transfer. For β-CD, we note that charge transfer occurs from the host to the guest in all three forms. Within the three forms, the charge transfer is

dx.doi.org/10.1021/jp403476n | J. Phys. Chem. B 2013, 117, 8603−8610

slightly larger (by ~0.02 a.u.) when the benzimidazole part is encapsulated as compared to the pyridyl part. Further, the charge transfer decreases in the following order **C** > **T** > **N** consistent with our binding energy predictions.

5. CONCLUSION

The protonation−deprotonation equilibria of 4PBI are significantly altered upon inclusion in cyclodextrin cavities. The orientation of dye in the inclusion complex is such that hydrogen bonds are formed between the dye and the primary/secondary −OH group. Hydrophobic interaction plays a major role as well. The pyridyl nitrogen of the dye can abstract protons from the hydroxyl groups inside the CD cavity, and thus, the proton transfer can occur even in the hydrophobic environment inside the CD cavity, provided the binding is loose, so that there is some space between the hydroxyl group and the pyridyl nitrogen. The driving force behind such proton abstraction is due to the fact that the basicity of the pyridyl nitrogen in the excited state is very high as compared with that in the ground state, when the complex is formed and protonation−deprotonation takes place. DFT calculations reveal that the insertion of 4PBI inside the CD is more feasible toward the pyridyl side rather than the benzimidazole side for a smaller cavity (α-CD). The complex can be stabilized by hydrogen bonding between the primary and secondary hydroxyl groups of CD and the benzimidazole nitrogen atoms of 4PBI and the interaction with the hydrophobic cavity of the host molecules.

■ ASSOCIATED CONTENT

Ⓢ Supporting Information

Additional absorption and fluorescence spectra and fluorescence decays. This material is available free of charge via the Internet at http://pubs.acs.org.

■ AUTHOR INFORMATION

Corresponding Authors

*E-mail: smahesh@barc.gov.in.

*Phone: +91 22 2576 7149, Fax: +91 22 2570 3480 E-mail: anindya@chem.iitb.ac.in.

Notes

The authors declare no competing financial interest.

■ ACKNOWLEDGMENTS

V.K. thanks CSIR for a Senior Research Fellowship. B.S. and M.S. thank Ajeya-Ameya systems of BARC for computing facilities. B.S. thanks Dr. Pradeepkumar K. S. and Dr. D. N. Sharma for their support.

■ REFERENCES

(1) Potter, C. A. S.; Brown, R. G. Excited-State Intramolecular Proton Transfer in Polar Solutions of 2-(2′-Hydroxyphenyl)-benzothiazole. *Chem. Phys. Lett.* **1988**, *153*, 7−12.

(2) Sinha, H. K.; Dogra, S. K. Electronic Spectra of Benzimidazolecarboxylic Acids: Effect of Solvents and Acid Concentrations. *Spectrochem. Acta, Part A* **1989**, *45*, 1289−1295.

(3) Sinha, H. K.; Dogra, S. K. Environmental Effects on the Absorption and Fluorescence Spectral Characteristics of Benzimidazole-2-carboxylic Acid and Its Ester. *Bull. Chem. Soc. Jpn.* **1989**, *62*, 2668−2675.

(4) Das, K.; Sarkar, N.; Ghosh, A. K.; Majumdar, D.; Nath, D. N.; Bhattacharyya, K. Excited-State Intramolecular Proton Transfer in 2-(2′-Hydroxyphenyl)benzimidazole and -benzoxazole: Effect of Rotamerism and Hydrogen Bonding. *J. Phys. Chem.* **1994**, *98*, 9126−9132.

(5) Douhal, A.; Amat-Guerri, F.; Acuna, A. U.; Yoshihara, K. Picosecond Vibrational Relaxation in the Excited-State Proton-Transfer of 2-(3′-Hydroxy-2′-naphthyl)benzimidazole. *Chem. Phys. Lett.* **1994**, *217*, 619−625.

(6) Rodriguez, M. C. R.; Mosquera, M.; Rodriguez-Prieto, F. Ground- and Excited-State Tautomerism in Anionic 2-(6′-Hydroxy-2′-pyridyl)benzimidazole: Role of Solvent and Temperature. *J. Phys. Chem. A* **2001**, *105*, 10249−10260.

(7) Flom, S. R.; Barbara, P. F. The Photodynamics of 2-(2′-Hydroxy-5′-methylphenyl)-benzotriazole in Low-Temperature Organic Glasses. *Chem. Phys. Lett.* **1983**, *94*, 488−493.

(8) Chudoba, C.; Riedle, E.; Pfeiffer, M.; Elsaesser, T. Vibrational Coherence in Ultrafast Excited State Proton Transfer. *Chem. Phys. Lett.* **1996**, *263*, 622−628.

(9) Rodriguez, M. C. R.; Rodriguez-Prieto, F.; Mosquera, M. Conformational Effects on the Photoinduced Proton-Transfer Processes in 1-Methyl-2-(3′-hydroxy-2′-pyridyl)benzimidazole. *Phys. Chem. Chem. Phys.* **1999**, *1*, 253−260.

(10) Takeuchi, S.; Tahara, T. Femtosecond Ultraviolet−Visible Fluorescence Study of the Excited-State Proton-Transfer Reaction of 7-Azaindole Dimer. *J. Phys. Chem. A* **1998**, *102*, 7740−7753.

(11) Rodriguez-Prieto, F.; Mosquera, M.; Novo, M. Dual Fluorescence of 2-(2′-Pyridyl)benzimidazole in Aqueous Solution due to Photoinduced Proton-Transfer Processes. *J. Phys. Chem.* **1990**, *94*, 8536−8542.

(12) Novo, M.; Mosquera, M.; Rodriguez-Prieto, F. Excited-State Behavior of 2-(4′-Pyridyl)benzimidazole in Aqueous Solution: Proton-Transfer Processes and Dual Fluorescence. *J. Phys. Chem.* **1995**, *99*, 14726−14732.

(13) Novo, M.; Mosquera, M.; Prieto, F. R. Prototropic Equilibria of 2-Pyridylbenzimidazoles in Aqueous Solution. *Can. J. Chem.* **1992**, *70*, 823−827.

(14) Khorwal, V.; Datta, A. Ground and Excited State Prototropism of 2-(4′-Pyridyl)benzimidazole in Micelles. *J. Photochem. Photobiol., A* **2012**, *250*, 99−102.

(15) Rath, M. C.; Palit, D. K.; Mukherjee, T. Effects of Organised Media on the Excited-State Proton Transfer in 2-(2′-Pyridyl)-benzimidazole. *J. Chem. Soc, Faraday Trans.* **1998**, *94*, 1189−1195.

(16) Mukherjee, T. K.; Ahuja, P.; Koner, A. L.; Datta, A. ESPT of 2-(2′-Pyridyl)benzimidazole at the Micelle−Water Interface: Selective Enhancement and Slow Dynamics with Sodium Dodecyl Sulfate. *J. Phys. Chem. B* **2005**, *109*, 12567−12573.

(17) Mukherjee, T. K.; Panda, D.; Datta, A. Excited-State Proton Transfer of 2-(2′-Pyridyl)benzimidazole in Microemulsions: Selective Enhancement and Slow Dynamics in Aerosol OT Reverse Micelles with an Aqueous Core. *J. Phys. Chem. B* **2005**, *109*, 18895−18901.

(18) Mukherjee, T. K.; Datta, A. Regulation of the Extent and Dynamics of Excited-State Proton Transfer in 2-(2′-Pyridyl)-benzimidazole in Nafion Membranes by Cation Exchange. *J. Phys. Chem. B* **2006**, *110*, 2611−2617.

(19) Dass, C. R.; Jessup, W.; Apolipoprotein, A.-I. Cyclodextrins and Liposomes as Potential Drugs for the Reversal of Atherosclerosis. A Review. *J. Pharm. Pharmacol.* **2000**, *52*, 731−761.

(20) Li, S.; Purdy, W. C. Cyclodextrins and Their Applications in Analytical Chemistry. *Chem. Rev.* **1992**, *92*, 1457−1470.

(21) Valle, E. M. M. D. Cyclodextrins and Their Uses: a Review. *Process Biochem.* **2004**, *39*, 1033−1046.

(22) Shizuka, H.; Fukushima, M.; Fuju, T.; Kobayashi, T.; Ohtani, H.; Hoshino, M. Proton-Induced Quenching of Methoxynaphthalenes Studied by Laser Flash Photolysis and Inclusion Effect of β-Cyclodextrin on the Quenching. *Bull. Chem. Soc. Jpn.* **1985**, *58*, 2107−2112.

(23) Breslow, R.; Dong, S. D. Biomimetic Reactions Catalyzed by Cyclodextrins and Their Derivatives. *Chem. Rev.* **1998**, *98*, 1997−2011.

(24) Szejtli, J. Downstream Processing Using Cyclodextrins. *Trends Biotechnol.* **1989**, *7*, 170−174.

(25) Takahashi, K. Organic Reactions Mediated by Cyclodextrins. *Chem. Rev.* **1998**, *98*, 2013−2033.
(26) Rekharsky, M. V.; Inoue, Y. Complexation Thermodynamics of Cyclodextrins. *Chem. Rev.* **1998**, *98*, 1875−1917.
(27) Zhang, X.; Gramlich, G.; Wang, X.; Nau, W. M. A Joint Structural, Kinetic, and Thermodynamic Investigation of Substituent Effects on Host−Guest Complexation of Bicyclic Azoalkanes by β-Cyclodextrin. *J. Am. Chem. Soc.* **2002**, *124*, 254−263.
(28) Szejtli, J. Utilization of Cyclodextrins in Industrial Products and Processes. *J. Mater. Chem.* **1997**, *7*, 575−587.
(29) Chachisvilis, M.; Garcia-Ochoa, I.; Douhal, A.; Zewail, A. H. Femtochemistry in Nanocavities: Dissociation, Recombination and Vibrational Cooling of Iodine in Cyclodextrin. *Chem. Phys. Lett.* **1998**, *293*, 153−159.
(30) Bortolus, P.; Monti, S. Cis ⇄ Trans Photoisomerization of Azobenzene-Cyclodextrin Inclusion Complexes. *J. Phys. Chem.* **1987**, *91*, 5046−5050.
(31) Hashimoto, S.; Thomas, J. K. Fluorescence Study of Pyrene and Naphthalene in Cyclodextrin-Amphiphile Complex Systems. *J. Am. Chem. Soc.* **1985**, *107*, 4655−4662.
(32) Cline-Love, L. J.; Grayeski, M. L.; Noroski, J.; Weinberger, R. Room-Temperature Phosphorescence, Sensitized Phosphorescence and Fluorescence of Licit and Illicit Drugs Enhanced by Organized Media. *Anal. Chim. Acta* **1985**, *170*, 3−12.
(33) Femia, R. A.; Scypinski, S.; Cline-Love, L. J. Fluorescence Characteristics of Polychlorinated Biphenyl Isomers in Cyclodextrin Media. *Enuiron. Sci. Technol.* **1985**, *19*, 155−159.
(34) Mishra, P. P.; Adhikary, R.; Lahiri, P.; Datta, A. Chlorin P6 as a Fluorescent Probe for the Investigation of Surfactant−Cyclodextrin Interactions. *Photochem. Photobiol. Sci.* **2006**, *5*, 741−747.
(35) Burai, T. N.; Panda, D.; Datta, A. Fluorescence Enhancement of Epicocconone in Its Complexes with Cyclodextrins. *Chem. Phys. Lett.* **2008**, *455*, 42−46.
(36) Singh, P. K.; Kumbhakar, M.; Pal, H.; Nath, S. Confined Ultrafast Torsional Dynamics of Thioflavin-T in a Nanocavity. *Phys. Chem. Chem. Phys.* **2011**, *13*, 8008−8014.
(37) Loftsson, T.; Duchene, D. Cyclodextrins and Their Pharmaceutical Applications. *Int. J. Pharm.* **2007**, *329*, 1−11.
(38) Funasaki, N.; Ishikawa, S.; Neya, S. Advances in Physical Chemistry and Pharmaceutical Applications of Cyclodextrins. *Pure Appl. Chem.* **2008**, *80*, 1511−1524.
(39) Rasheed, A.; Ashok Kumar, C. K.; Sravanthi, V. V. N. S. S. Cyclodextrins as Drug Carrier Molecule: A Review. *Sci. Pharm.* **2008**, *76*, 567−598.
(40) Loftsson, T.; Brewster, M. E. Pharmaceutical Applications of Cyclodextrins. 1. Drug Solubilization and Stabilization. *J. Pharm. Sci.* **1996**, *85*, 1017−1025.
(41) Shaikh, M.; Mohanty, J.; Sundararajan, M.; Basikuttan, A. C.; Pal, H. Supramolecular Host−Guest Interactions of Oxazine-1 Dye with β- and γ-Cyclodextrins: A Photophysical and Quantum Chemical Study. *J. Phys. Chem. B* **2012**, *116*, 12450−12459.
(42) Yoruzu, T.; Hoshino, M.; Imamura, M.; Shizuka, H. Photo-excited Inclusion Complexes of Beta-Naphthol with Alpha-, Beta-, and Gamma-Cyclodextrins in Aqueous Solutions. *J. Phys. Chem.* **1982**, *86*, 4422−4426.
(43) Jung, M. H.; Park, J. M.; Lee, I.-Y. C.; Ahn, M. Synthesis of 2-(1-Methyl-1,2,5,6-tetrahydropyridin-3-yl)benzimidazoles. *J. Heterocyclic Chem.* **2003**, *40*, 37−44.
(44) Mishra, P. P.; Koner, A. L.; Datta, A. Interaction of Lucifer Yellow with Cetyltrimethyl Ammonium Bromide Micelles and the Consequent Suppression of Its Non-Radiative Processes. *Chem. Phys. Lett.* **2004**, *400*, 128−132.
(45) TURBOMOLE V6.0 2009, a Development of University of Karlsruhe and Forschungszentrum Karlsruhe GmbH, 1989−2007, TURBOMOLE GmbH, since 2007; available from http://www.turbomole.com.